

# PRELIMINARY IMPEDANCE BUDGET FOR NSLS-II STORAGE RING\*

Alexei Blednykh<sup>#</sup> and Samuel Krinsky  
 BNL, Upton, NY, 11973-5000, U.S.A.

## Abstract

The wakefield and impedance produced by the components of the NSLS-II storage ring have been computed for an electron bunch length of 3mm rms. The results are summarized in a table giving for each component, the loss factor ( $\kappa_{||}$ ), the imaginary part of the longitudinal impedance at low frequency divided by the revolution harmonic ( $\text{Im}Z_{||}/n$ ), and the transverse kick factors ( $\kappa_x, \kappa_y$ ).

## INTRODUCTION

In order to be able to accurately estimate the instability threshold currents in the NSLS-II storage ring, it is necessary to have a reliable model of the ring impedance. In this note, we report work in progress aimed at evaluating the ring impedance. Extensive calculations of the impedance and wakefields produced by the components of the vacuum vessel have been performed using the electromagnetic simulator GdfidL [1]. Our results for the loss factor ( $\kappa_{||}$ ), the imaginary part of the longitudinal impedance at low frequency divided by the revolution harmonic ( $\text{Im}Z_{||}/n$ ), and the transverse kick factors ( $\kappa_x, \kappa_y$ ) are summarized in Table 1.

## STORAGE RING COMPONENTS

### Vacuum Chambers

The impedance of the NSLS-II vacuum chambers is discussed ref. [2]. The regular aluminum vacuum chamber has elliptical cross-section with inner dimensions of full-width  $2a=76\text{mm}$  and full height  $2b=25\text{mm}$ . In the dipole magnets there is an exit slot of 15mm full-height and in the multipoles there is a slot of 10mm full-height. Of particular concern is the impedance of the special large aperture infrared chambers which have a full-width of 134mm and a full-height of 67mm. Each IR chamber contains a large vertical aperture port with a mirror near the electron beam.

### Aluminum Resistive Wall

In order to estimate the resistive wall impedance, we introduce a simplified model. We consider the 780m circumference to be comprised of 720m of the aluminum vacuum chamber with elliptical cross-section described above and 20 in-vacuum undulators of 3m-length with copper chamber having 5 mm vertical full-gap. In actuality the vacuum vessel is more complicated and the final configuration of insertion devices is not yet decided. We feel this simple model will give a reasonable first

estimate of the resistive wall contribution to the ring impedance. More detailed calculations will be made in the future.

### Photon Absorber

To protect the vacuum chamber and insertion devices in the ring from damage due to synchrotron radiation, photon absorbers (Fig. 1) are used. The model consists of a regular elliptical beampipe with 50 mm width and 25 mm height, with a rectangular slot 10 mm high, 180 mm long, and 180 mm deep. A triangular copper burr is located inside the slot for synchrotron radiation absorption. It projects 5 mm inside the regular elliptical beampipe.

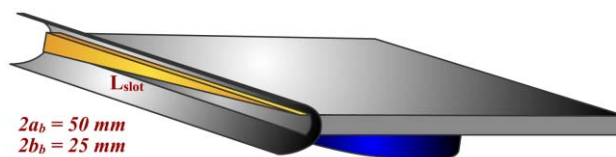


Figure 1: Photon Absorber.

### Beam Position Monitor

Due to excitation of resonant modes in the buttons of the beam position monitors (Fig. 2), the impedance, kick factor, and loss factor depend very strongly on the BPM button geometry. The BPM button geometry can be optimized to reduce impedance contribution and heating, without losing its resolution. To estimate BPM contribution to the transverse and longitudinal impedance, buttons designed for the SOLEIL BPM were modeled on the regular elliptic beampipe for NSLS-II. Results of the transverse impedance were compared with results for the SOLEIL BPM geometry [3]; in both cases, 50  $\Omega/\text{m}$  was computed.

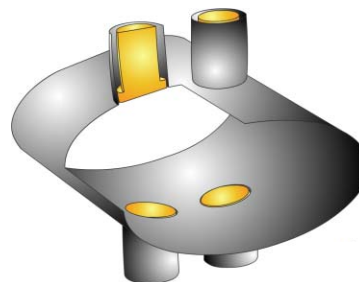


Figure 2: Beam Position Monitor (BPM).

### Horizontal Scraper

It is planned to install scrapers to eliminate outlying electrons to protect the permanent magnet undulators. From the impedance estimations of other laboratories, horizontal or vertical beam scrapers (Fig. 3) can produce impedance comparable with that of a rectangular step or a tapered transition with a large angle of opening. Two

\*Work supported by DOE contract DE-AC02-98CH10886.

<sup>#</sup>blednykh@bnl.gov

horizontal scrapers of the presented geometry are under consideration for application in the NSLS-II ring. Two vertical scrapers are also planned.



Figure 3: Horizontal Scraper.

### CESR-B RF Cavity Assembly

Investigation of longitudinal and transverse impedances of cavities and transitions [4,5] has begun, using simplified geometries. The first approximation simplifies the geometry of a single cavity as currently installed in the Cornell Electron Storage Ring, CESR. The 3D model of the 500 MHz CESR-B [6] assembly is shown in Fig. 4. Its length is 2.6 m. The geometry consists of the single 500 MHz RF main cavity with the attached, round, 120 mm radius on one side, and the fluted beampipe for HOM coupling on the other. Inside the round beampipe, close to the transition on both sides of the structure, ferrite material is located for HOM damping.

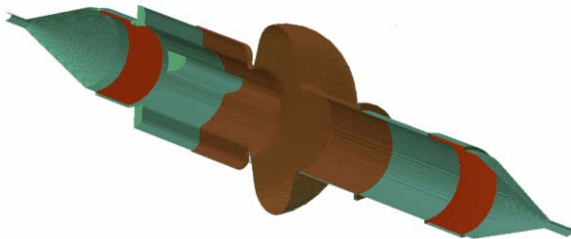


Figure 4: 3D Model of CESR-B Cavity Assembly in GdfidL.

The broad-band impedance in the whole assembly can be estimated as a sum of cavity and transition impedances. In Table 1 we present data separately for the 500 MHz CESR-B main RF cavity and for a third-harmonic cavity derived by reducing the dimensions of the CESR-B main RF cavity by a factor of 3. Two main and two harmonic cavities will be located in one 8m straight section. "Cavity transitions" in Table 1 refers to set of tapered transitions per straight between the regular vacuum chamber and the main cavity ( $L_{Taper}=300\text{mm}$ ), the round main cavity beam pipe and the round harmonic cavity beam pipe ( $L_{Taper}=300\text{mm}$ ) and the round harmonic cavity pipe and the regular vacuum chamber ( $L_{Taper}=100\text{mm}$ ).

### Cryo-Permanent Magnet Undulator Chamber

A 3D model of the cryo-permanent magnet undulator (CPMU) is shown in Fig. 5. The device consists of two magnet arrays of width  $w_m = 100$  mm and thickness 34 mm, located inside a rectangular vacuum chamber of

width  $w_{vc} = 180$  mm and height  $h_{vc} = 170$  mm [7]. The tapered transition consists of two parts: 1) a fixed portion between the regular beampipe and the undulator vacuum chamber; and 2) a flexible-height portion with one end fixed to the interior of the undulator vacuum chamber and the other end fixed to the moveable magnet array. The flexible portion only consists of flat upper and lower conductive plates with no side walls. For simplicity in the 3D model, we used a continuous smooth taper of length 180 mm. Also, due to mesh limitations, we have shortened the magnet section length to 0.5 m.

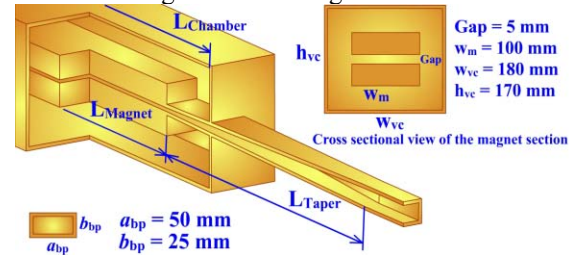


Figure 5: Cryo-Permanent Magnet Undulator Chamber.

### Superconducting Undulator Chamber

The results of wakepotential and impedance investigations for the tapered elliptic vacuum chamber (Fig. 6) for the superconducting undulator (SCU) were already published in [7, 8 and 9] for the two different taper lengths 180mm and 500mm. The tapers provide a smooth transition between the magnet section and the regular beam pipe. Wakepotential and impedance depend very strongly on taper angle and chamber width. The width of the current design of the regular elliptic vacuum chamber for NSLS-II is 76 mm. According to this, data for the tapered elliptic vacuum chamber in Table 1 are presented for the geometry with a taper length  $L_{Taper}=180\text{mm}$  between the magnet section of major axis  $2a_s=15\text{mm}$  and minor axis  $2b_s=5\text{mm}$  and the regular beam pipe of major axis  $2a_b=76\text{mm}$  and minor axis  $2b_b=25\text{mm}$ .

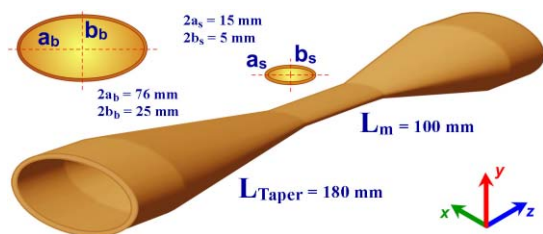


Figure 6: Superconducting Undulator Chamber.

## CONCLUSION

Impedance analysis of accelerator components is continuing. Special attention will be paid to the RF assembly, CPMU chambers and infra-red beam extraction chambers.

The far-IR large gap dipole chamber is currently under design at NSLS-II. The special concern is resonant modes (narrow-band impedance) due to IR extraction mirror and the short-range wakepotential (broad-band impedance) due to the tapered transition.

Table 1: Calculated impedance for components of the NSLS-II storage ring. <sup>1</sup>Values for bellows and flanges were calculated by R. Nagaoka [10] for SOLEIL with  $\sigma_s = 6$  mm. <sup>2</sup>Values for 9mm bunch length. The other geometric impedances were calculated with  $\sigma_s = 3$  mm. The bunch-length dependence of the wakefields will be determined in future work. \*ease – extreme anomalous skin effect [4].

Object	Number of occurrences	$\kappa_{  }$ , [V/pC]	$(\text{Im}Z_{  }/n)_0$ , [ $\Omega$ ]	$\kappa_x$ , [V/pC/m]	$\kappa_y$ , [V/pC/m]
Absorber	180	$3.4 \times 10^{-3}$	$9.2 \times 10^{-6}$	0.5	0.002
Bellows <sup>1</sup>	180	$8.7 \times 10^{-3}$	$124 \times 10^{-6}$	0.8	2
BPM	270	$20 \times 10^{-3}$	$47 \times 10^{-6}$	0.9	1.1
Cavity transitions/straight	2	3.5	$14 \times 10^{-3}$	25.4	57
500 MHz CESR-B cavity	4	0.31	$40 \times 10^{-3}$	0.17	0.17
1500 MHz CESR-B cavity	4	0.52	$13.4 \times 10^{-3}$	2.6	2.6
Dipole chamber	60	$3.3 \times 10^{-5}$	$0.7 \times 10^{-7}$	$4.5 \times 10^{-3}$	0
Quad. and Sext. chamber	90	$0.5 \times 10^{-5}$	$0.1 \times 10^{-7}$	$0.7 \times 10^{-3}$	0
Flange <sup>1</sup>	300	$0.47 \times 10^{-3}$	$16 \times 10^{-6}$	0.141	0.141
Injection Region	1	TBD	TBD	TBD	TBD
SCU chamber geometric	TBD	$22.6 \times 10^{-3}$	$0.6 \times 10^{-3}$	61	257
SCU chamber ease* (2.5m)	TBD	$5.6 \times 10^{-3}$		13	26
IR chamber <sup>2</sup>	4	$2.6 \times 10^{-3}$	$0.8 \times 10^{-3}$	2	8.1
CPMU geometric	TBD	$95 \times 10^{-3}$	$1.1 \times 10^{-3}$	136	425
CPMU resistive wall (3.5m)	TBD	$66 \times 10^{-3}$		112	225
720m Al resistive wall	1	4.0		272	545
Scraper (Horizontal)	2	0.22	$1.4 \times 10^{-3}$	22	2
Scraper (Vertical)	2	TBD	TBD	TBD	TBD

The CPMU chamber has a complex geometry. Its kick factor value is comparable with the value of the resistive wall for 720m. It is the largest geometric kick factor per component. The narrow-band impedance of the structure depends on the cross-sectional geometry of the vacuum enclosure and the length of the magnet.

The RF cavity assembly was studied component by component. The largest contribution to the longitudinal impedance comes from the tapered transitions. Based on GdfidL computations, ferrite material does not affect the short-range wakepotential.

The impedance budget for NSLS-II will be evaluated and renewed with ongoing changes in component geometries.

## REFERENCES

[1] W. Bruns, GdfidL, <http://www.gdfidl.de>  
 [2] A. Blednykh and S. Krinsky, "Impedance of Electron Vacuum Chambers for the NSLS-II Storage Ring", PAC2007.

[3] R. Nagaoka, Private communication.  
 [4] Conceptual design report for NSLS-II p. 780, <http://www.nsls2.bnl.gov>.  
 [5] A. Blednykh, S. Krinsky and J. Rose, "Coupling impedance of CESR-B RF cavity for the NSLS-II storage ring" PAC 2007.  
 [6] H. Padamsee et al. "Accelerating Cavity Development for the Cornell B-Factory, CESR-B", PAC1991, May 6-9, Sun Francisco, pp786.  
 [7] A. Blednykh, S. Krinsky, B. Podobedov and J.-M. Wang, "Transverse Impedance of Small-Gap Undulators for NSLS-II", EPAC 2006, Edinburgh, UK 26-30 June 2006.  
 [8] A. Blednykh and J.-M. Wang, "A Model Study of Transverse Mode Coupling Instability at NSLS-II", PAC2005, Knoxville, Tennessee, 2005.  
 [9] A. Blednykh, "Trapped Modes in an Elliptic Vacuum Chamber", Nucl. Instrum. Meth. A. 565, 2006.  
 [10] R. Nagaoka, "Numerical Evaluation of Geometric Impedance for SOLEIL," Proc. EPAC2004, 2038.